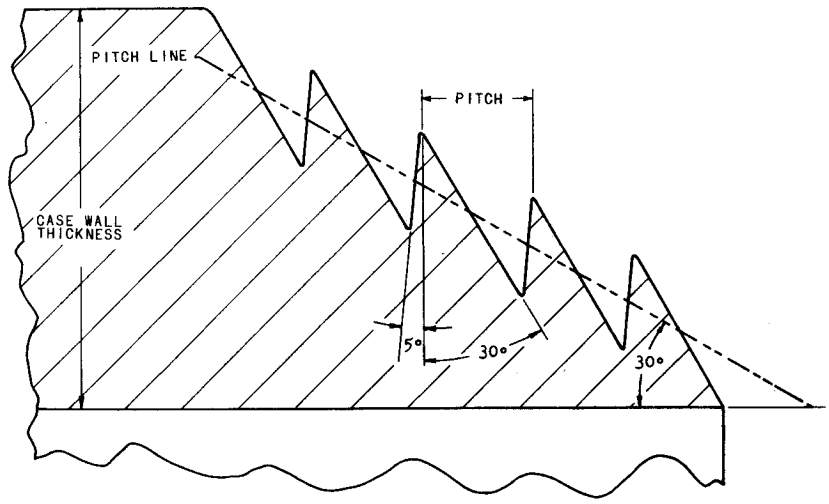

Fig. 4 Spiral buttress thread.

creases approximately 12% during the 4.7-sec burn times. The major wall erosion is beneath the slots, as would be expected.

Headcap Attachment Method

External strain rods were used to retain a metal headcap for the demonstration tests. However, some work has already been performed on molded threads as a method of retaining the headcap, and the concept appears to be feasible. This unique molded thread, for which a patent is pending, is called a Spiral Buttress Thread.

The basic form of the Spiral Buttress Thread is shown in Fig. 4. The principal advantages of this inherently high-strength thread are that it can be easily molded and it maintains the longitudinal physical properties of molded cylinders without changing the diametral or wall-thickness dimensions. Additional advantages are that full engagement of the thread, regardless of its length or diameter, can be made with less than one revolution of the mating parts, the thread is score- and jam-proof, and perfect alignment of threaded parts is automatic on assembly.

The Spiral Buttress Threads have been molded in the forward end of the feasibility rocket motor. Hydrostatic burst tests have been performed on these threaded cases in the same manner as previously described. Currently, thread failures are occurring at 90% of the case burst pressures.

Summary

The demonstration tests have revealed that integrally-molded rocket motor cases and nozzles are feasible as sounding rocket boosters. The cost study conducted by Stanford Research Institute further shows that a molded meteorological sounding rocket could be produced in large quantities at considerably lower costs than current marketable motors. The cost savings have been achieved through the elimination of several customary motor operations and reduction in manpower requirements. The unique thread design also contributes greatly to the feasibility of molding these low-cost motors.

Table 1 Cost summary[a]

Inert parts	
Asbestos phenolic molding compound	$ 80.00
Nozzle insert	2.00
Assembly hardware	2.00
Molding labor	15.00
Finishing labor	9.00
Molding facilities write-off	25.00
Propellant loading	
Propellant ingredients	30.25
Propellant loading	21.00
Motor finishing labor	7.00
Handling and casting fixtures write-off	10.00
Igniter and payload separation ordnance	
Materials and labor	38.15
Total	$239.40

[a] Contract NAS7-773 by Stanford Research Institute based on 12,000 units over a 4-yr period.

Use of Fibers in Gravity-Gradient Stabilization Systems

SUBHASH GARG* AND PETER HUGHES†
University of Toronto, Toronto, Ontario, Canada

1. Introduction

AN enormous literature now exists on gravity-gradient (GG) stabilization of Earth-pointing satellites.[1] This principle can be successfully implemented only on satellites having large linear dimensions, and these have been traditionally imparted via extensible metallic "booms" that are storable for later extension in orbit. As is well known, these slender booms are subject to both static and dynamic distortions because of differential thermal expansion of the metal, and their interaction with solar radiation pressure may raise difficulties.

An alternative, in the case of booms aligned with the local vertical, is to replace them with a thin inextensible fiber with a tip mass at the end.[2] The gravity-gradient forces acting outward on the tip mass will keep the fiber taut, which is then akin to a rigid boom as regards the resultant inertia distribution. Now thermal distortion can be eliminated by proper choice of material. Also, the flexible fiber can be made extremely thin, all but eliminating the radiation pressure effects. Solar forces remain on the tip masses and the main body, but if these are spherical and the configuration is symmetrical,

Received March 3, 1971; revision received June 1, 1971. Supported in part by the National Research Council of Canada (Grant A-4183) and United States Air Force Office of Scientific Research (Grant AF-AFOSR 68-1490).

Index category: Spacecraft Attitude Dynamics and Control.

* Research Assistant, Institute for Aerospace Studies.

† Associate Professor, Institute for Aerospace Studies. Associate Member AIAA.

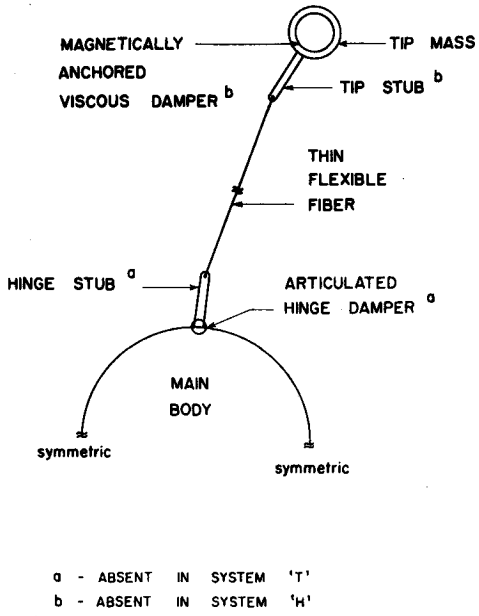

Fig. 1 General configuration showing both hinge and tip dampers.

the resultant torque can be made to vanish simply by choosing the area to mass ratio equal for all bodies.[2]

In this paper a design utilizing this concept is proposed. A linearized analysis is carried out in the orbital plane only. This implies that sufficient lateral damping is present to prevent the pitching motion from rendering the null roll-yaw condition unstable and causing significant pitch/lateral coupling. Two damping schemes are considered—one of these is the magnetically-anchored damper[4] (this also causes a weak coupling that is ignored here). The other scheme is an articulated hinge damper.[3] Their relative merits are evaluated and optimization techniques are used to demonstrate feasibility in a synchronous equatorial orbit.

2. Configuration

Essentially the proposed design is as shown in Fig. 1. Symmetry is dictated by the synchronous altitude application. Basically, tip masses are appended to two fibers connected to the main body so as to stay aligned with the local vertical in the undisturbed state. Consideration of the damping schemes shows that this is not enough. For example, the fiber, lacking rigidity, cannot be used in an articulated hinge. Hence a short, rigid stub is inserted between the fiber and the satellite body. A hinge damper can then be used to dissipate the relative motion between the stub and the satellite body. A spring also may be included to augment the GG "stiffness" if such proves beneficial.

The flexibility of the fibers keeps the tip masses quite free to rotate about their own axes without causing an appreciable torque on the main body. Especially if dampers are located in the tip masses, it is expected that their torque will not be as effective in damping the body motion, or even the fiber motion, as in damping the rotation of the tip mass alone.‡ This was confirmed by studying the motion of a simple pendulum with a linear damper located in the bob, in a GG-type force field.[2] It was found that the swinging mode of the pendulum is indeed very poorly damped in comparison to the motion of the pendulum bob about its own axis. The pendulum model also showed that if another short rigid stub is attached to the tip mass it increases the coupling between the swinging and the rotational modes; this leads to good damping of the former. An optimization of the pendulum

‡ Pointed out to the authors by B. Etkin, University of Toronto.

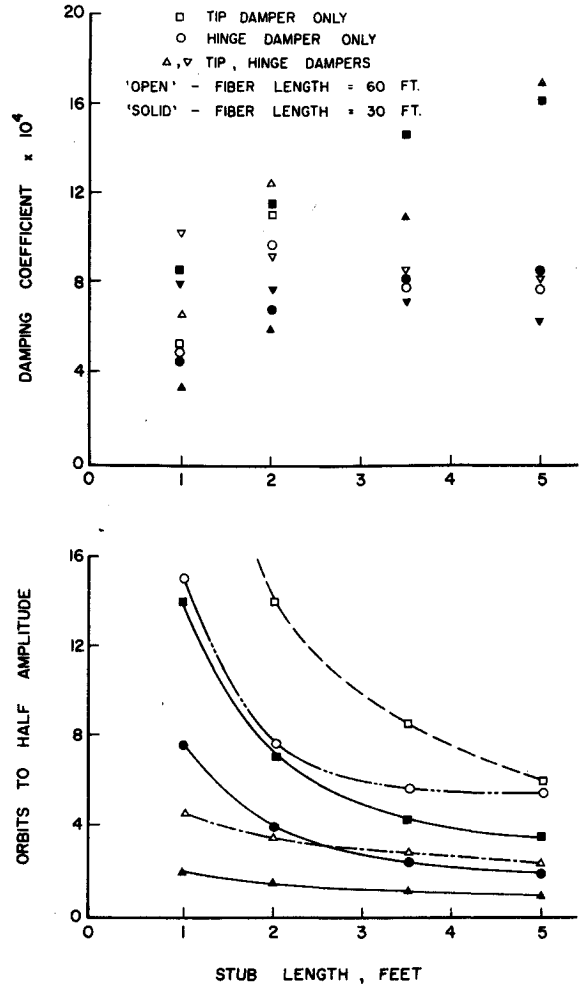

Fig. 2 Time taken for a disturbance in the least-damped mode to damp out to half amplitude, and corresponding damping coefficients.

parameters showed, as expected, that the longer the stub is made, the better is the performance, so a tip stub is incorporated into the design along with the tip damper.

The most general configuration thus has both hinge and tip dampers. It has seven degrees of freedom in pitch. Two other configurations result if only the tip damper alone or only the hinge damper alone is used, and only the corresponding stubs are retained. These three configurations are abbreviated as systems *HT*, *T*, and *H* respectively. Their performance is compared below.

3. Equations of Motion and Solution

Equations for small-angle motion were obtained using the Lagrangian formulation, with the relative angular displacements of the constituent bodies as generalized coordinates in the orbital frame. The stubs and fibers were taken as massless and all dampers were considered linear. The orbit was assumed to be nominally circular with a small eccentricity which appears as a disturbing torque.[3] Torques due to radiation pressure were made to vanish by choosing the tip area properly (Ref. 2, Sec. 2.25). Details of the derivation are given elsewhere.[2] The form of the equations is as follows:

$$\mathbf{M}\boldsymbol{\theta}'' + \mathbf{D}\boldsymbol{\theta}' + \mathbf{K}\boldsymbol{\theta} = \mathbf{g} \qquad (1)$$

where primes denote differentiation with respect to the true anomaly, which is the independent variable. Here $\boldsymbol{\theta}$ is the state vector, $\mathbf{g}$ is the disturbing torque vector, and $\mathbf{M}$, $\mathbf{D}$, $\mathbf{K}$

are 7×7 matrices for system HT and 5×5 matrices for systems H and T. $\mathbf{D}$ is symmetric with damping elements and is positive semidefinite. $\mathbf{K}$ is symmetric with gravity-gradient "spring" elements and is positive definite. $\mathbf{M}$ contains terms of the dimensions of moment of inertia, and is positive definite in general. However, if some degrees of freedom have no mass associated with them, as in the present model, the corresponding generalized coordinates will be ignorable, and $\mathbf{M}$ will be only semidefinite. It can be shown that if, in Eq. (1), $\mathbf{M}$ has rank $p < n$ where n is the number of coordinates, the system can be reduced to p equations of the form of Eq. (1) and $n - p$ additional first-order equations, by elementary transformations on Eq. (1) and the vector $\boldsymbol{\theta}$. Equivalently, a reduced set of generalized coordinates may be found such that the corresponding inertia matrix is nonsingular. However, none of these transformations affect the $n + p$ eigenvalues of the system, and since in this stability study only the eigenvalues were to be calculated, the equations have been left in the form of Eq. (1) with $\mathbf{M}$ singular.

For actual computation it is possible to decouple Eq. (1) into two independent sets, corresponding to libration angles describing the "symmetric" and "antisymmetric" oscillatory modes. The characteristic roots of the system are unaffected by this transformation. They are obtained as the roots of the polynomial

$$\det (s^2\mathbf{M} + s\mathbf{D} + \mathbf{K}) = 0 \qquad (2)$$

Care must be taken in the numerical solution of Eq. (2), due to the fact that $\mathbf{M}$ is only semidefinite, so that the order is $(n + p)$ instead of $2n$, and $(n - p)$ leading coefficients of Eq. (2) are zero. The steady-state response to eccentricity torques, which are periodic of the form $\mathbf{a}e \sin\gamma$, is also computed. It is of the form $\mathbf{b} \sin(\gamma + \phi)$, where $\mathbf{b}$ and ϕ are obtained by direct substitution into Eq. (1) and some matrix operations. This is made easier by the fact that eccentricity excites only the symmetric modes.

The full expansion of Eqs. (1) and (2) is somewhat complicated and lengthy and does not offer much additional insight. It is therefore omitted here and the interested reader is referred to Ref. 2.

4. Optimization and Constraints

Performance of the satellites depends on geometrical (fiber and stub lengths) and dynamical parameters (mass, damping coefficients), for a given main body weight and radius. To facilitate comparison the systems are optimized using steepest descent. The performance index is the time for an impulsive disturbance, applied in the least-damped mode, to damp out to half of its initial amplitude. This corresponds to the maximum real part of the system eigenvalues.

Initial optimization studies disclosed several things. First, including a hinge spring always degraded the performance, so it was dropped. Second, keeping the fiber plus stub length constant, the fiber length invariably tended to zero while the stub length increased to the maximum permitted. This happened for all three systems, indicating the fiber length to be an adverse parameter. Therefore, lower limits were imposed on the fiber length and upper limits were placed on the stub lengths, in keeping with the motivation for this study, namely, to reduce solar pressure and thermal effects. Third, in some cases the tip mass decreased excessively, invalidating the "taut fiber" assumption. So a lower limit was placed on the tip mass. Thus we have inequality constraints on all parameters except the damping coefficients.

These inequalities were satisfied by prohibiting values of the parameters outside the constraint boundary. Some other modifications were made to the ordinary steepest descent method to improve convergence. Details of these and a discussion of the performance of the programs may be found in Ref. 2.

5. Results

Only a summary of the results is presented here. Full results are available in Ref. 2, except for system H which was not analyzed therein.

Values for the constraint boundaries are as follows: tip mass 2.0 lb, fiber lengths 30 ft and 60 ft; for each fiber length, stub lengths less than 1, 2, 3.5, and 5 ft, respectively. Thus there are 8 cases for each system. For HT, where two stubs are present, these values apply to the tip stub, the hinge stub constraint being 3 ft in all cases. These somewhat arbitrary values were chosen to illustrate salient features of the systems. In all cases the stub lengths and fiber length took on values at the constraint boundary. The tip mass hit the boundary in 23 out of 32 cases considered. Almost all optima were characterized by root coalescence.

The performance index is shown in Fig. 2 vs the constrained stub length for the three systems, with the fiber length as a parameter. It is seen that system HT, using both dampers, performs the best. System T with only tip damping is largely ineffective, as the tip damper has relatively little influence on the main body. But system H with hinge dampers only is a happy compromise, since the hinge damper is more simple to mechanize, and does not introduce any pitch/lateral coupling. The rapid "flattening out" of the curves makes the use of fibers worthwhile, as there is no point in increasing the stub length any further. Damping times near 2 orbits can be obtained using the hinge damper alone.

The damping coefficients at the optimum are also shown in Fig. 2, plotted similarly. In general, these show a predictable pattern. More damping is required when the fiber length is increased. The optimum damping coefficient changes markedly as the corresponding stub length is allowed to increase, showing the close interrelationship.

Behavior of parameters such as the tip mass and tip body radius is omitted here. Pointing error amplitudes in response to an orbital eccentricity of 0.01 were also computed and were always of the order of 1° for the main body, and even less for other components. The use of fibers thus does not entail a compromise in pointing performance.

6. Conclusions

The main conclusions of this paper can be summarized thus: 1) Gravity-gradient designs using fibers to replace a large portion of the conventional booms are feasible as shown by an example. 2) Use of fibers necessarily entails some deterioration of transient damping performance. However, this is not necessarily true for pointing performance. 3) An articulated hinge damper is much better suited to a fiber design than a tip damper. Better performance is possible by combining both but at the expense of increased rigid stub/fiber length ratio.

These conclusions are based on a preliminary study only and show the basic design concept to be promising.

References

[1] *Proceedings of the Symposium on Passive Gravity-Gradient Stabilization*, NASA SP-107, 1965.

[2] Garg, S. C., "On the Use of Flexible Strings in Gravity-Gradient Stabilization Systems," TN 135, June 1969, Univ. of Toronto, Inst. of Aerospace Studies, Toronto, Ontario, Canada.

[3] Etkin, B., "Dynamics of Gravity-Oriented Systems With Application to Passive Stabilization," *AIAA Journal*, Vol. 2, No. 6, June 1964, pp. 1008–1014.

[4] Katucki, K. J. and Moyer, R. G., "Systems Analysis and Design of a Class of Gravity-Gradient Satellites Utilizing Viscous Coupling Between the Earth's Magnetic and Gravity Fields," NASA SP-107, 1965, pp. 55–72.